

2021

Review of Humidity Effect on Humid Air-to-Water Condensation by a Cooling Surface for Atmospheric Water Harvesting

Gyeong Sung Kim
University of Maryland

Tao Cao
University of Maryland, taocao@umd.edu

Yunho Hwang

Follow this and additional works at: <https://docs.lib.purdue.edu/iracc>

Kim, Gyeong Sung; Cao, Tao; and Hwang, Yunho, "Review of Humidity Effect on Humid Air-to-Water Condensation by a Cooling Surface for Atmospheric Water Harvesting" (2021). *International Refrigeration and Air Conditioning Conference*. Paper 2163.
<https://docs.lib.purdue.edu/iracc/2163>

This document has been made available through Purdue e-Pubs, a service of the Purdue University Libraries. Please contact epubs@purdue.edu for additional information. Complete proceedings may be acquired in print and on CD-ROM directly from the Ray W. Herrick Laboratories at <https://engineering.purdue.edu/Herrick/Events/orderlit.html>

Review of Humidity Effects on Humid Air-Water Condensation by a Cooling Surface for Atmospheric Water Harvesting

Gyeong Sung KIM¹, Tao CAO¹, Yunho HWANG^{1*}

¹ 4164 Glenn Martin Hall Bldg., Center for Environmental Energy Engineering
Department of Mechanical Engineering, University of Maryland,
College Park, MD., 20742, United States

* Corresponding Author. Tel: (301) 405-5247, email: yhhwang@umd.edu

ABSTRACT

Many atmospheric water harvesting technologies have been produced to mitigate water scarcity as an auxiliary source of water. These technologies may be described as direct and indirect water collection techniques. The direct method is to induce a phase-change turning from vapor to liquid on a cooling surface and generate condensate without interim processes. On the other hand, the indirect method has absorption or adsorption processes to take water from humid air before producing water. This paper focuses on the direct methods and discusses the effects of humidity and surface temperature on water generation rates and condensate droplet formation patterns in a macro- and micro-view with previous experimental data. In the view of water harvesting, the generation rate of condensate showed a dependency on the temperature difference between a dew point and a surface temperature. As a result of analyzing droplet formation behaviors considering the importance of the subcooling effect in the macro-view, it was investigated that droplet formation rates and the growth regimes of the condensate also had strong relationships with the humidity of air and the surface temperature. This review would be useful for further research on the modeling of condensate droplet formation and condensation enhancement for thermally driven water generation systems.

Keywords: Atmospheric water, relative humidity, drop-wise condensation, dew point, water harvesting

1. INTRODUCTION

Recently, a technology of atmospheric water harvesting (AWH) has shown a possibility as a new water source to mitigate water scarcity in an arid area since the convenience of shipping and deployment to respond quickly to the locations where electric grids and freshwater are unreliable. Many types of devices, which handle water vapor differently, have been developed so far. These technologies can be classified into a direct and an indirect water collection method, as Table 1 shows. The direct method is to use a cooling surface and generate condensate on its surface without any interim processes. On the other hand, the indirect method has an interim process such as absorption or adsorption to take water vapor from humid air before producing water. In this study, we focused on the direct condensation method rather than the indirect AWH.

Condensation of water vapor is crucial not only to AWH but also to many industrial sectors, such as desalination, power plants, and dehumidification systems. Condensation may occur in two ways, film condensation (FWC) and drop-wise condensation (DWC). In general, it is known that the heat transfer coefficient (HTC) of DWC is around 5-7 times higher than that of FWC (Eslami and Elliott, 2011; Rose, 2002; Rykaczewski and Scott, 2011; Koch *et al.*, 1997; Schmidt *et al.*, 1930). Therefore, many techniques for direct water harvesting or condensation enhancement have been focused on avoiding droplets spreading out over surfaces and lasting DWC by improving the geometry or the wettability of the surface.

Early applications used plates, tubes, and fins, but these methods are still attractive to many researchers seeking functionally long-lasting and simple devices. For morphology improvement of a condensing surface, observing the critical droplet size on the micro-grooved surfaces was explored by Sommers and Jacobi (2008). The experimental research results showed the droplet volume at incipient sliding on the micro-grooved was significantly reduced by more than 50% compared to droplets on plain surfaces. Shi *et al.* (2018) showed that thin string could enhance the

water collection rate in fog water harvesting, and they found that the fog-harvesting rate increased with decreasing wire diameter of the collecting materials.

Table 1: Atmospheric water harvesting technologies

Direct or indirect	Technique	Detail method	Reference	
Direct method: Surface cooling	Various morphology	Thin drainage path	Lee <i>et al.</i> (2012)	
		Micro-grooved	Sommers and Jacobi (2008)	
		String	Shi <i>et al.</i> (2018)	
	Surface coating	Graphene coating	Preston <i>et al.</i> (2015)	
		Biomimetic micro-patterned coating	Thickett <i>et al.</i> (2011)	
		Various morphology and wettability improvement	Mesh-covered hydrophobic	Wen <i>et al.</i> (2018)
			Hydrophobic nanostructure	Miljkovic <i>et al.</i> (2012)
	Other	Needle with hybrid surface	Mondal <i>et al.</i> (2015)	
		Hydrophobic nanowire composition	Wen <i>et al.</i> (2017)	
		Electrospray with cooling surface	Reznikoy <i>et al.</i> (2015)	
Indirect method: Material use	Liquid absorption	Liquid desiccant	Gido <i>et al.</i> (2016)	
		Membrane-based absorption	Huang and Zhang (2013)	
	Solid adsorption	Solid desiccant coated HX	Li <i>et al.</i> (2016)	
		Metal-organic framework	Kim <i>et al.</i> (2018)	

For wettability, Lee *et al.* (2012) examined the condensation rate of humid air in DWC with a uniformly hydrophilic surface and relatively lower wettability surfaces. They showed the hydrophilic surface exhibited higher rates of water condensation and collection than the lower wettability ones. However, it is not easy to maintain the DWC with a hydrophilic surface. Therefore, the wettability modification by using hydrophobic or hybrid (hydrophobic-hydrophilic) materials to achieve faster droplet growth or quicker droplet removal has been performed by many researchers. Preston *et al.* (2015) developed and tested ultrathin scalable chemical vapor deposited (CVD) graphene coatings to enhance DWC. Their study demonstrated that the ultrathin CVD graphene coatings promoted drop-wise condensation, and they claimed the heat transfer performance was improved by 4 times higher than that measured for FWC on plain copper plate. Thickett *et al.* (2011) have studied animals living in dry climates for the direct harvesting method. They developed the coating mimicking the *Stenocara* beetle and tested the biomimetic micropatterned surfaces along with different types of films concerning the volume and generation rate of condensate water.

Some researchers performed improvement of both wettability and geometry. Miljkovic *et al.* (2012) investigated condensation on superhydrophobic nanostructured surfaces, and they observed the droplet growth and shedding behavior to find the overall performance enhancement in comparison to a hydrophobic plain surface. In the experiment, they showed heat flux enhancement for partially wetting droplet morphologies. Hybrid superhydrophobic-hydrophilic surfaces with impaling a superhydrophobic film on an array of steel needles were tested by Mondal *et al.* (2015), and they showed condensation rates with different needle pitches and different tilt angle of the surface. Wen *et al.* (2018) tested superhydrophobic hierarchical mesh-covered surface for drop-wise condensation and presented an achievement of faster droplet growth rate and smaller droplet departure compared to other hydrophobic plain and structured surfaces. To achieve rapid droplet removal, Wen *et al.* (2017) developed nano-wired surfaces. The experimental study showed that the overall heat flux of a nanostructure surface was 100 % higher than a plain hydrophobic surface. Aside from this, electrostatic enhancement of phase-change processes was applied by Reznikov *et al.* (2015) to improve heat exchange during condensation. They demonstrated an up to 7.5 mL/hr water harvesting rate with the 1:613 scale prototype moisture harvester at 11 watts of reduced cooling power to the condenser.

Although many condensation technologies have been developed concerning the droplet creation on a cooling surface and generation enhancement, it has not yet been fully clarified. Thus, the purpose of this paper is to investigate how the humidity affects the atmospheric water generation in a macro view and the droplet creating formulations in a micro view by analyzing data from previous studies to provide another approach. Furthermore, the water droplet creation patterns under different humidity were discussed based on specific experimental data.

2. MATERIALS AND METHODS

Most of the experimental data in this paper were selected only from humid air condensation research performed under atmospheric pressure. Thus, the bulk steam condensation process and forced convective cases, including condensations with windy circumstances, were not considered. To review the previous research data, the missing properties of humid air such as a saturation temperature (or dew point temperature), a saturation vapor pressure, and partial vapor pressure were calculated by using Engineering Equation Solver (EES) (Klein, 2019). Also, missing values of atmospheric pressures in the empirical studies were considered as 101.325 kPa for property estimation.

3. HUMIDITY EFFECTS ON SURFACE CONDENSATION RATE

3.1 Humidity and Overall Mass Transfer Coefficient with Phase Change

The cooling temperature of the surface should be below the dew point of the humid air to produce water, and it can be provided by coolants, a vapor compression cycle, or a Peltier effect. The dew point is the temperature at which water vapor has reached the saturation point (100% relative humidity, RH) (ANSI/ASHRAE Standards 41.6, 2006). Thus, when humid air contacting a cooling surface reaches its dew point, the water vapor of the humid air starts to be condensed. The dew point varies according to the temperature and the humidity of the air. Figure 1 shows the dew point changes with the RH at different air temperatures under the atmospheric pressure. At the same RH, the higher dew point means that the humid air holds more amount of moisture itself. Therefore, the dew point may be considered as a direct value to estimate how much water it contains and will be produced from an atmospheric water generator.

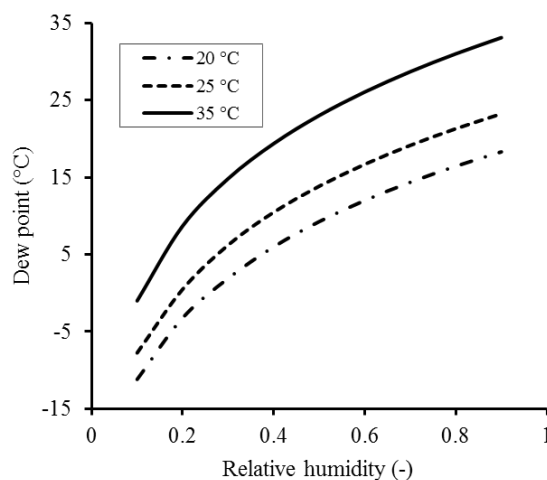


Figure 1. Dew point temperature for ambient air at 20 °C, 25 °C, and 35 °C as a function of relative humidity (calculated by EES assuming the atmospheric pressure as 101.325 kPa)

Regarding the saturation temperature or dew point of humid air, the water generation rate (\dot{m}) on the unit area of a cooling surface by using the temperature difference between the saturation temperature of humid air and cooling surface temperature can be defined as Eq. (1) shows (Çengel and Ghajar, 2015).

$$\dot{m} = \frac{q''}{h'_{fg}} = \frac{\bar{h}_L(T_{sat} - T_s)}{h'_{fg}} \quad (1)$$

q'' is the heat flux per unit area to the surface and h'_{fg} is the modified latent heat. \bar{h}_L is the average heat transfer coefficient, and T_{sat} and T_s are the saturation temperature of humid air and the cooling surface temperature, respectively.

Rohsenow (1956) introduced the modified latent heat to account for the cooling of liquid below the saturation temperature as Eq. (2) where $c_{p,l}$ is the specific heat of the liquid.

$$h'_{fg} = h_{fg} + 0.68c_{p,l}(T_{sat} - T_s) \quad (2)$$

The average heat transfer coefficient, \bar{h}_L , over entire heat exchanger is determined by the geometry, the wettability, the flow rate of the condensate and the humid air, and so on. Therefore, using Eq. (1) to estimate the condensate generation rate (\dot{m}) requires pre-definition for each term. However, in a real life, the geometry and the wettability of an atmospheric water generator or a heat exchanger are fixed once installed. Also, the range of temperature and RH of ambient air can be assumed that they are generally maintained 10-40 °C and 0.1-1, respectively. Thus, it may be worthy to observe if Eq. (1) can be defined by using overall heat transfer coefficient (HTC) for quick estimation of the condensate generation rate.

To simplify Eqs. (1) and (2), the latent contribution of the overall HTC with phase change may be used. Therefore, the total condensation rate per unit area may then be determined by HTC, subcooling ($T_{sat} - T_s$), and latent heat of water from vapor to liquid phase (Eq. (3)).

$$\dot{m} = HTC \frac{(T_{sat} - T_s)}{h_{fg}} \quad (3)$$

For the condensation rate as a function of the temperature difference as shown in Eq. (3), Baghel et al.'s experimental study (2020) showed that the condensation rate on hydrophobic surfaces increased almost linearly as the temperature difference between the saturation temperature and the surface temperature. For another case, Gao (2012)'s experimental result was reviewed. The researcher performed the atmospheric water harvesting tests under the different coolant flow rates at 0.65, 0.85, 1.05, 1.25, and 1.45 L·s⁻¹ and measured the total mass of the condensate from the dehumidifier. The water generation data was rearranged as a function of the temperature difference of the dew point and the coolant inlet temperature (Fig. 2(a)) based on the assumption that the coolant temperature is not different from the condensing surface temperature. As a result of the data review, it can be considered the condensate generation rate and the temperature difference is in a proportional relationship. The data of the coolant flow rate higher than 1.05 L·s⁻¹ was extracted as Fig. 2(b) shows to consider the more constant surface temperature of the dehumidifier, and it clearly shows the linearity between the subcooling temperature and condensate generation rate. Therefore, the condensate generation rate may be considered to be proportional to the difference between dew point and surface temperature, and the HTC of humid ambient air to estimate the condensate generation rate can be assumed to be constant.

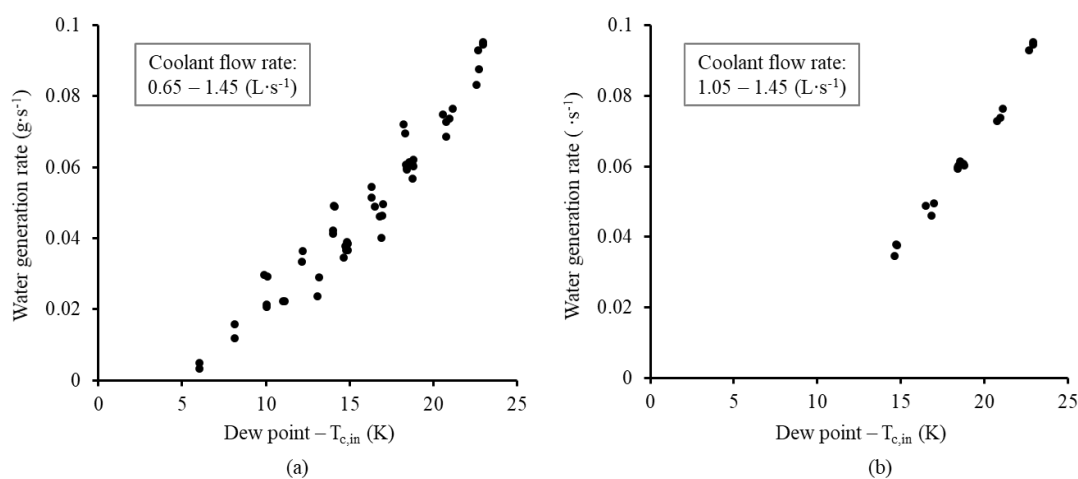


Figure 2. Water generation rate with temperature difference between dew point and coolant (data source: Gao, 2012), (a) 0.65 - 1.45 L·s⁻¹ of coolant flow rate, (b) 1.05 - 1.45 L·s⁻¹ of coolant flow rate

3.2 Review of Advanced AWH Technology

Several papers were reviewed to examine the water production rates of AWH using advanced technologies, as Fig. 3 shows. For the analysis, the atmospheric pressure was assumed to be 101.325 kPa for the cases that did not mention it. Ghosh *et al.* (2014) performed condensation tests of the bioinspired-patterned surface, the straight-line patterned surface, and the plain aluminum plate in 80% of constant RH air with 20 °C and 35 °C of ambient temperatures, respectively. They cooled down the specimen with a Peltier device and compared the condensation rate of each specimen. Al-Khayat *et al.* (2017) developed and carried out different patterned polymer coatings to harvest water from the moist air of 20.3 °C dry bulb temperature and 95% RH. Mondal *et al.* (2015) investigated the water collection rate of hybrid superhydrophobic-hydrophilic surfaces attached to 300 μm height of needles and tested under 70 % RH with different needle tip temperatures over 10-14 hours. Gupta *et al.* (2018) examined the condensation rate with hydrophilic surfaces, which were maintained constant surface temperature 8 °C by Peltier-heat sink system and different humidities.

As the illustration for the comparison of condensate generation rate (Fig. 3) shows, each advanced technology may be characterized by the overall heat transfer coefficient (HTC) which is defined by Eq. (3). The latent heat h_{fg} of Eq. (3) varies along with the saturation temperature, but the variation is very small. For example, the difference of the latent heats at 40 °C and at 0 °C of a dew point is less than 4%. For the ambient air, furthermore, it is rare for the dew point to change sharply. Thus, it may not be a big issue to consider h_{fg} to be a constant value when a production rate of condensate from ambient air is reviewed.

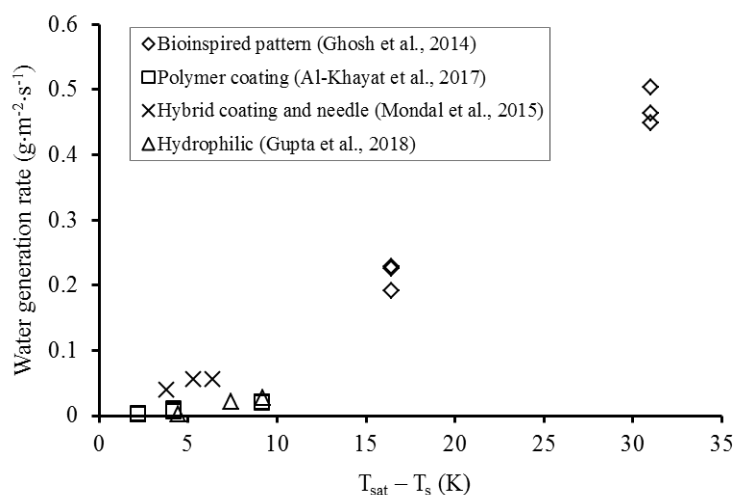


Figure 3: Comparison of condensate generation rate from humid air as a function of subcooling

However, it is still hard to conclude which technology in Fig. 3 could generate more water from humid air under the same conditions, because Baghel *et al.* (2020) showed the variation of condensation rate with different saturation temperatures (303K and 313K) and the same subcooling conditions. Therefore, more studies are needed on the relationship between humidity and condensation rate for the direct performance comparison of test results in Fig. 3.

4. HUMIDITY EFFECTS ON CONDENSATE DROPLET FORMATION

4.1 Subcooling and Condensate Droplet Formation Regime

Many researchers have also focused on condensate droplet formation as the DWC is preferred over FWC owing to the higher HTC. For the droplet growth on a cooling surface, it has been known that it follows power laws as Eq. (4) shows, and generally two distinguishable regimes are observed (e. g. $\mu_1 \neq \mu_2$) (Viovy *et al.*, 1988, Beysens, 1995, Lo *et al.*, 2014, Castillo *et al.*, 2015, and Kajiya *et al.*, 2016).

$$\langle r \rangle \sim t^{\mu_i} \quad (4)$$

where $\langle r \rangle$ is the average droplet radius, and t is time after nucleation. μ_i is the exponent of each growth regime, and the value indicates the growth speed of each regime. Interestingly, the power of the first regime was smaller than that of the second regime's (e. g. $\mu_1 < \mu_2$) according to previous experimental research results (Lo *et al.*, 2014, Castillo *et al.*, 2015, and Kajiya *et al.*, 2016). The first regime occurs after nucleation has occurred and is characterized as a growth regime without significant interactions between drops. The first regime shows a low surface coverage, which is the ratio of area covered by droplets and cooling surface area. Meanwhile, the second regime leads to interactions by coalescence between the droplets (Beysens,1995).

Castillo *et al.* (2015) and Pionnier *et al.* (2018) performed condensation tests with different RHs of humid air and showed different power values of Eq. (4) according to the RHs. According to their experimental results, the general growth pattern on the same cooling surface over time and humidity was dependent on the RH. Chavan *et al.* (2016) performed vapor condensation tests on a hydrophobic and a superhydrophobic surface and measured the exponent value of Eq. (4). Interestingly, Castillo *et al.* (2015) observed the same value of the slope of each second regime during their tests with different RHs. They examined the average-radius growth behavior of the condensate water droplets for the four different RH cases. They observed the distribution and growth of condensate droplets at four different relative humidities (45%, 50%, 55%, and 70%) with constant temperatures of the surface and humid air ($T_s = 5\text{ }^\circ\text{C}$, $T_a = 20\text{ }^\circ\text{C}$). Similarly, Chavan *et al.* (2016) showed the same exponent values for the second regimes of the droplet condensation tests with different surface materials. They investigated the droplet growth rate on a hydrophobic and superhydrophobic surface during condensation. As a result, they had 0.1 and 0.2 for a hydrophobic and a superhydrophobic surface, respectively, in the first regime (μ_1) while the second regimes (μ_2) of them are the same values as 0.5. To analyze the humidity effect on droplet condensation in depth, Castillo *et al.*'s test results were reviewed, focusing on each inflection point and departing point. Two regimes were distinguished for four different RHs, and a strong dependency between the RH of each case and growth rate was revealed as Fig. 4 (a) shows. To analyze the relationship between RH and the growth rate of droplets on a cooling surface, the nucleation point (O), each inflection point (A, B, C, and D) between the first and the second regime, and departing points (A*, B*, C*, and D*) of Fig. 4(a) were examined with considering the temperature difference between the saturation temperature and the surface temperature. For this analysis, the atmospheric pressure of the humid air was assumed to be 101.325 kPa. As a result of the analytical review, the ending time of each regime and ΔT were strongly related to each other as Fig. 4 (b) and (c) show. In addition, the fraction of the time for the first regime (t_{μ_1}) and the total growth time ($t_{\mu_1} + t_{\mu_2}$) was calculated by Eq. (5) (example: $\alpha_A = \ln(t(OA)) / \ln(t(OAA^*))$) in Fig. 4 (a)), and the result is illustrated at Fig. 4 (d).

$$\alpha = \frac{\ln(t_{\mu_1})}{\ln(t_{\mu_1} + t_{\mu_2})} \quad (5)$$

Based on the relationship of each time frame of the regime in Fig. 4 (d), the time fraction of regime (α) was reversely proportional to the subcooling temperature, ΔT . Though further experimental studies are necessary, it may be considered as every smooth condensing surface has its own constant α while condensate droplets are formatted.

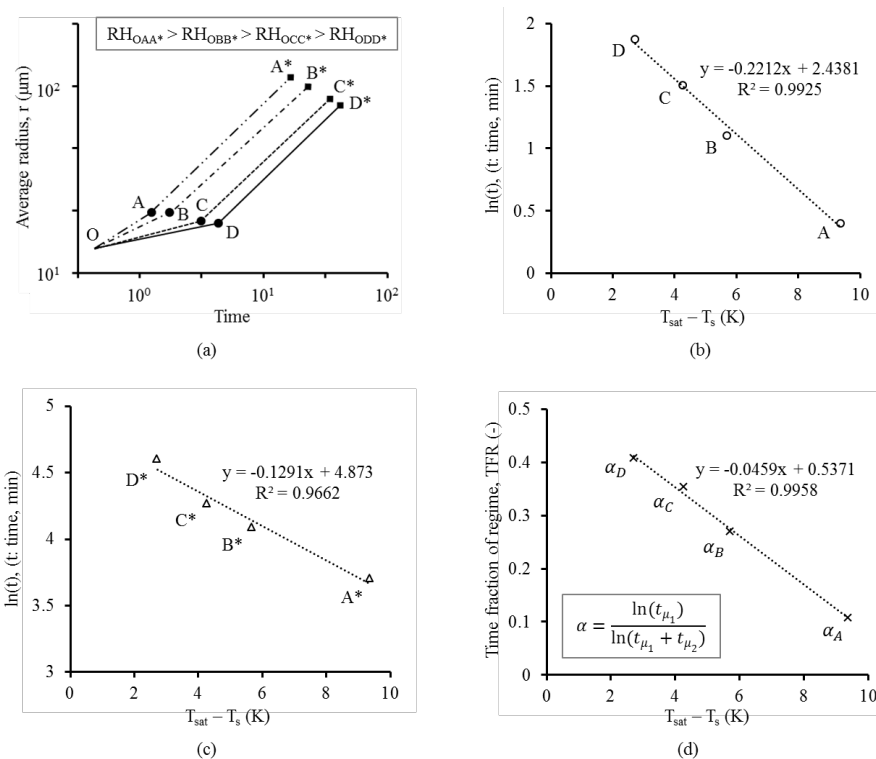


Figure 4: Analytical review of water droplet growth pattern based on the test results of Castillo *et al.* (2015) (a) general growth pattern on a same cooling surface over time and humidity (b) time period of the first regime vs. subcooling (c) full time period of the first and second regimes vs. subcooling (d) time fraction of regime vs. subcooling

4.2 Humidity and Condensate Droplet Formation Rate

Graham and Griffith (1973) were interested in droplet size distributions in drop-wise condensation. They found significantly larger drop populations at atmospheric pressures than low pressures. Furthermore, they presented approximately 10% of the cooling surface was bare, and 50 percent of the heat was transferred through 5% of the surface area for both atmospheric and low-pressure conditions. Castillo *et al.* (2015) showed another notable experimental result which can determine the condensate droplet formation rate of different sizes. They investigated the condensation rate per unit surface area of a single droplet as a function of droplet radius at different RH conditions. Based upon their study assuming that all droplet shapes were hemisphere on the surface, the formation rate of each droplet size per unit area ($N(r) \cdot \text{m}^{-2} \cdot \text{s}^{-1}$) was calculated and illustrated as Fig. 5 shows. For example, 100 μm of the droplet could be created as many as approximate 3.07×10^4 of droplets per square meter per second at 45 % RH. Thus, the droplet creation rate can be defined as Eq. (6).

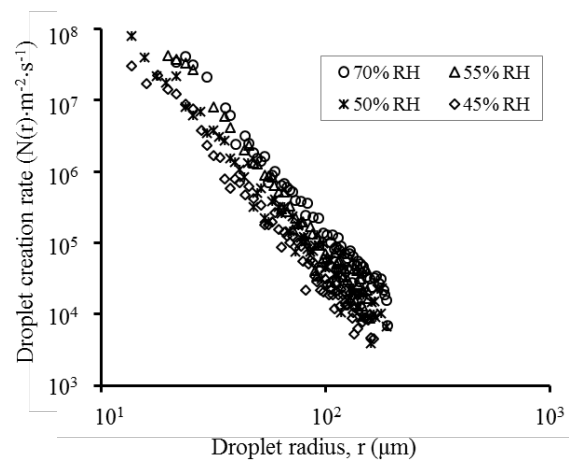


Figure 5: Formation rate of each droplet size per unit area at different humidity conditions (the original figure: Castillo *et al.* (2015)).

$$a_H \cdot \ln(\dot{n}(r) \cdot r^k) = C \quad (6)$$

where a_H is a constant depending on the relative humidity, $\dot{n}(r)$ is the creation number of its size of droplet per unit area per unit time ($N(r) \cdot m^{-2} \cdot s^{-1}$), r is the radius (μm) of droplet. In addition, Eq. (5) can be expressed as Eq. (6)

$$\ln(\dot{n}(r) \cdot r^k) = C_H \quad (6)$$

According to the analytical review of Castillo's test results, C_H value was greater in higher humidity of air than lower humidity of air, and k was approximate 3.68 for their test.

6. CONCLUSIONS

Condensation of water vapor of humid air is exploited in atmospheric water harvesting, dehumidification of HVAC systems, distillation and desalination, and other industrial sectors since increasing an HTC and performance efficiency in a condensation process means saving energy and reducing initial capital and operational costs. Thus, it is desirable to achieve DWC in industrial applications, and for this reason, many researchers have been focusing on developing novel technologies (e.g., surface coating, geometry modification, and nano-material composition) that can last drop-wise status during a condensation process.

However, predicting the condensate generation rate from a condenser sometimes requires many analyzing steps and assumptions. Thus, this paper reviewed how the humidity and cooling surface temperature affect the atmospheric water generation and the droplet growth rate in a macro-view to simply estimate the condensate generation rate in a humid air handling process. According to previous experimental studies, the condensate generation rate may be regarded as a proportional relationship with the temperature difference between the dew point and the surface temperature.

This paper also reviewed the condensate droplet formation in a micro-view to consider humidity effects. By studying droplet growth rates considering different RH levels, many researchers found that the theoretical exponent depends on the RH and the wettability of the cooling surface. They observed an increase of the exponent of the first regime while that of the second regime, which appears when coalescence occurs, was constant and not impacted by the RH and the wettability of the surface. Though further experimental studies are required, the droplet growth behavior can be defined by the ambient humidity and temperature because the droplet formation regime shows a strong dependency on its dew point and surface temperature. Thus, this analytical study on the relationship between subcooling and condensate droplet formation in this review could serve as guidelines for further research on modeling a water generation rate from humid air and improvement of a water vapor condensation process.

NOMENCLATURE

α	time fraction of regime	(-)
DBT	dry bulb temperature	(°C)
h_{fg}	latent heat of water vapor	(kJ·kg ⁻¹)
h'_{fg}	modified latent heat of water vapor	(kJ·kg ⁻¹)
HTC	overall heat transfer coefficient	(W·m ⁻² ·K ⁻¹)
\dot{m}	total condensation rate per unit area	(g·m ⁻² ·s ⁻¹)
\dot{n}	droplet creation rate	(#·m ⁻² ·s ⁻¹)
r	radius	(μm)
q''	heat flux per unit area	(W·m ⁻²)
$\langle r \rangle$	average of droplet radius	(m)
t	time	(s)
T	temperature	(K)

Subscript

H	humidity
i	droplet formation regime
s	cooling surface
sat	saturation

REFERENCES

- [1] Al-Khayat, O., Hong, J. K., Bec, D. M., Minett, A. I., and Neto, C. (2017). Patterned polymer coatings increase the efficiency of dew harvesting. *ACS Applied Material and Interfaces*, 9, 13676-13684.
- [2] ANSI/ASHRAE Standard 41.6-1994. (2006). *Standard Method for Measurement of Moist Air Properties*, 1791 Tullie Circle NE, Atlanta, ASHRAE.
- [3] Baghel, V., Basant, S.S., and Muralidhar, K. (2020). Dropwise Condensation from Moist Air over a Hydrophobic Metallic Substrate. *Applied Thermal Engineering* 181, 115733.
- [4] Çengel, Y.A. and Ghajar, A.J. (2015). *Heat and Mass Transfer: Fundamental and Application (5th Eds)*, 614-637. New York, NY: McGraw-Hill Education.
- [5] Castillo, J. E., Weibel, J. A., and Garimella, S. V. (2015). The effect of relative humidity on drop-wise condensation dynamics. *International Journal of Heat and Mass Transfer*, 80, 759-766.
- [6] Eslami, F., and Elliott, J. A. W. (2011). Thermodynamic Investigation of the Barrier for Heterogeneous Nucleation on a Fluid Surface in Comparison with a Rigid Surface. *Journal of Physical Chemistry, B*(115), 10646-10653.
- [7] Gao, Z. (2012). *Dehumidification of greenhouses in cold regions*. Master degree thesis. University of Saskatchewan.
- [8] Ghosh, A., Beaini, S., Zhang, B. J., Ganguly, R., and Megaridis, C. M. (2014). Enhancing drop-wise condensation through bioinspired wettability patterning, *Langmuir*, 30, 13103-13115.
- [9] Gido, B., Friedler, E., and Broday, D. M. (2016). Liquid-desiccant vapor separation reduces the energy requirements of atmospheric moisture harvesting. *Environmental Science and Technology*, 50, 8362-8367.
- [10] Graham, C., and Griffith, P. (1973). Drop Size Distributions and Heat Transfer in Dropwise Condensation. *International Journal of Heat and Mass Transfer* 16(2), 337-46.
- [11] Gupta, R., Das, C., Roy, A., Ganguly, R., and Datta, A. (2018). Arduino based temperature and humidity control for condensation on wettability engineered surfaces. *Emerging Trends in Electronic Devices and Computational Techniques (EDCT)*, 1-6.
- [12] Huang, S.M., and Zhang, L.Z. (2013). Researches and trends in membrane-based liquid desiccant air dehumidification. *Renewable and Sustainable Energy Reviews*, 28, 425-440.
- [13] Jang, Y. J., Choi, D. J., Lee, Y. G., and Kim, S. (2015). Experimental study of condensation heat transfer in the presence of noncondensable gas on the vertical tube. *Proceedings of the KNS 2015 spring meeting*, (pp. 1CD-ROM). Korea, Republic of: KNS.
- [14] Kim, H., Rao, S. R., Kapustin, E. A., Zhao, L., Yang, S., Yaghi, O. M., and Wang, E. N. (2018). Adsorption-based atmospheric water harvesting device for arid climates. *Nature Communications*, 9, 1-8.

- [15] Klein, S. A. (2019). *EES: Engineering Equation Solver*, Academic Professional Version 10.644-3D, F-Chart Software.
- [16] Koch, G., Zhang, D. and Leipertz, A. (1997). Condensation of steam on the surface of hard coated copper discs. *Heat and Mass Transfer* 32, 149–156.
- [17] Lee, A., Moon, M.W., Lim, H., Kim, W.D., and Kim, H.Y. (2012). Water harvest via dewing. *Langmuir*, 28, 10183-10191.
- [18] Li, A., Thu, K., Ismail, A. B., Shahzad, M. W., and Kim, C. N. (2016). Performance of adsorbent-embedded heat exchangers using binder-coating method, *International Journal of Heat and Mass Transfer*, 92, 149–157.
- [19] Miljkovic, N., Enright, R., Nam, Y., Lopez, K., Dou, N., Sack, J. and Wang, E. N. (2013). Jumping-droplet-enhanced condensation on scalable superhydrophobic nanostructured Surfaces. *Nano Letters* 13 (1), 179-187.
- [20] Mondal, B., Eain, M. M. G., Xu, Q.F., Egan, V. M., Punch, J., and Lyons, A. M. (2015). Design and fabrication of a hybrid superhydrophobic–hydrophilic surface that exhibits stable drop-wise condensation, *ACS Applied Material and Interfaces*, 7, 23575-23588.
- [21] Pionnier, N., Barati, S. B., Contraires, E., Berger, R., Guibert, M., Benayoun, S., and Valette, S. (2018). Design of an Environment Controlled Dew Tracking Setup to Emphasize the Role of the Relative Humidity on Breath Figures Dynamics. *EPJ Techniques and Instrumentation* 5:2.
- [22] Preston, D. J., Mafra, D. L., Miljkovic, N., Kong, J., and Wang, E. N. (2015). Scalable Graphene Coatings for Enhanced Condensation Heat Transfer. *Nano Letters*, 15(5), 2902–2909.
- [23] Reznikov, M., Salazar, M., Lopez, M., and Rivera-Sustache, M. (2015). Electrically enhanced harvesting of water vapor from the air. *Proc. ESA Annual Meeting on Electrostatics 2015*, 1-11.
- [24] Rohsenow, W.M. (1956). Heat transfer and temperature distribution in laminar film condensation. *Trans. ASME*, 78, 1645-1648.
- [25] Rose, J. W. (2002). Dropwise condensation theory and experiment: A review. *Proceedings of the Institution of Mechanical Engineers, Part A: Journal of Power and Energy*, 216(2), 115-128.
- [26] Rykaczewski, K., and Scott J. H. J. (2011). Methodology for Imaging Nano-to-Microscale Water Condensation Dynamics on Complex Nanostructures. *Acs Nano*, 5, 5962-5968.
- [27] Schmidt, E., Schurig, W. and Sellschopp, W. (1930). Versuche über die Kondensation von Wasserdampf in Film- und Tropfenform. *Technische Mechanik und Thermodynamik* 1, 53–63.
- [28] Shi, W., Anderson, M. J., Tulkoff, J. b., Kennedy, B. S. and Boreyko, J. B. (2018). Fog harvesting with harps. *ACS Applied Materials and Interfaces* 10 (14), 11979-11986.
- [29] Sommers, A. D., and Jacobi A. M. (2008). Wetting phenomena on micro-grooved aluminum surfaces and modeling of the critical droplet size. *Journal of Colloid and Interface Science*, 328, 402–411.
- [30] Thickett, S. C., Chiara N., and Andrew T. H. (2011). Biomimetic surface coatings for atmospheric water capture prepared by dewetting of polymer films. *Advanced Materials* 23 (32), 3718–3722.
- [31] Viovy, J. L., Beysens, D., and Knobler, C. M. (1988). Scaling description for the growth of condensation patterns on surfaces. *Phys. Rev.A* 37, 4965–4970.
- [32] Wen, R., Li, Q., Wu, J., Wu, G., Wang, W., Chen, T., Ma, X., Zhao, D., and Yang, R. (2017). Hydrophobic copper nanowires for enhancing condensation heat transfer, *Nano Energy* 33, 177–183.
- [33] Wen, R., Xu, S., Zhao, D., Yang, L., Ma, X., Liu, W., Lee, Y.C., and Yang. R. (2018). Sustaining enhanced condensation on hierarchical mesh-covered surfaces. *National Science Review*, 878–887.

ACKNOWLEDGEMENT

We gratefully acknowledge the support of Korea Water Resources Corporation and the Center for Environmental Energy Engineering (CEEE) at the University of Maryland.